DOI: 10.1534/genetics.107.071621

Microhomology-Mediated End Joining in Fission Yeast Is Repressed by Pku70 and Relies on Genes Involved in Homologous Recombination

Anabelle Decottignies[1]

Cellular Genetics, Christian de Duve Institute of Cellular Pathology, Faculty of Medicine, Catholic University of Louvain, 1200 Brussels, Belgium

Manuscript received February 6, 2007
Accepted for publication April 26, 2007

ABSTRACT

Two DNA repair pathways are known to mediate DNA double-strand-break (DSB) repair: homologous recombination (HR) and nonhomologous end joining (NHEJ). In addition, a nonconservative backup pathway showing extensive nucleotide loss and relying on microhomologies at repair junctions was identified in NHEJ-deficient cells from a variety of organisms and found to be involved in chromosomal translocations. Here, an extrachromosomal assay was used to characterize this microhomology-mediated end-joining (MMEJ) mechanism in fission yeast. MMEJ was found to require at least five homologous nucleotides and its efficiency was decreased by the presence of nonhomologous nucleotides either within the overlapping sequences or at DSB ends. Exo1 exonuclease and Rad22, a Rad52 homolog, were required for repair, suggesting that MMEJ is related to the single-strand-annealing (SSA) pathway of HR. In addition, MMEJ-dependent repair of DSBs with discontinuous microhomologies was strictly dependent on Pol4, a PolX DNA polymerase. Although not strictly required, Msh2 and Pms1 mismatch repair proteins affected the pattern of MMEJ repair. Strikingly, Pku70 inhibited MMEJ and increased the minimal homology length required for efficient MMEJ. Overall, this study strongly suggests that MMEJ does not define a distinct DSB repair mechanism but reflects "micro-SSA."

ONE of the most toxic lesions to DNA is the double-strand break (DSB). If left unrepaired, DSB has the potential to disrupt genomic integrity. Notably, many cancers of lymphoid origin are due to defective DSB repair of V(D)J recombination intermediates (Jackson 2002). Cells have evolved two main pathways to repair DSBs: *n*on*h*omologous *e*nd *j*oining (NHEJ), a process resulting in direct resealing of the break without the need of extended homology between both ends, and *h*omologous *r*ecombination (HR), which, through at least 20 bp of homology (Shen and Huang 1986), repairs breaks by copying genetic information from either homologous chromosomes or sister chromatids. There are at least three different mechanisms of HR in mitotic cells: gene conversion (GC), break-induced replication, and single-strand annealing (SSA); the latter mechanism repairs DSBs arising between direct repeats of homology, leading to deletion of the intervening nucleotides (Paques and Haber 1999).

Genetic requirements for HR and NHEJ have been extensively investigated in a variety of organisms. In budding yeast, HR machinery includes genes from the *RAD52* epistasis group [*RAD52*, *RAD59*, *RAD51*, *RAD54*, *RAD55*, and *RAD57* (RAD51 family); *RDH54* and *RAD50*, *XRS2*, and *MRE11* (MRE11 family)] (Paques and Haber 1999). *RAD52* encodes a single-standed DNA (ssDNA)-binding protein with single-strand annealing activity required for all HR events, including SSA, although the requirement for *RAD52* in SSA diminishes as the length of homologous repeats flanking the DSB increases (>2 kb) (Ozenberger and Roeder 1991). Budding yeast *RAD59*, a *RAD52* homolog with strand-annealing activity, is also required for SSA, especially when the homologous regions are short (Sugawara *et al.* 2000; Davis and Symington 2001). On the other hand, the ATP-dependent strand exchange mediator Rad51, the homolog of bacterial RecA, is required for GC and the majority of break-induced replication events but not for SSA in budding yeast (Paques and Haber 1999; Davis and Symington 2004). The involvement of the *Saccharomyces cerevisiae* Mre11 complex (RAD50/XRS2/MRE11) in HR is still controversial although the DNA end-bridging activity of Rad50 could potentially stimulate HR (D'Amours and Jackson 2002). In *Schizosaccharomyces pombe*, it was suggested that Rad50 stimulates sister-chromatid recombination but not recombination between homologous chromosomes (Hartsuiker *et al.* 2001). Key proteins for NHEJ are the heterodimeric DNA-binding proteins Ku70/Ku80 and DNA ligase IV (Jackson 2002). The Ku70/80 heterodimer is required for efficient and accurate NHEJ; it binds DNA ends and protects them from exonuclease digestion (Getts and Stamato 1994). Accordingly,

[1]*Address for correspondence:* ICP, Faculty of Medicine, Catholic University of Louvain, Avenue Hippocrate, 74+3, 1200 Brussels, Belgium. E-mail: anabelle.decottignies@gece.ucl.ac.be

cells lacking Ku show decreased efficiency in nonhomologous DSB repair and increased nucleotide loss at repair junctions.

A decade ago, extrachromosomal (EC) DSB repair studies in budding yeast *YKU70*-deficient cells provided the first evidence for the existence of an alternative end-joining pathway (Boulton and Jackson 1996). Repair junctions recovered from *yku70*Δ cells were characterized by nucleotide deletion and overlapping microhomologies (3–16 bp) (Boulton and Jackson 1996). The term microhomology-mediated end joining (MMEJ) has been proposed for this DNA repair pathway. Strikingly, this Ku-independent MMEJ pathway was highly reminiscent of a major DSB repair mechanism operating in mammalian cells since short stretches of homologous nucleotides (1–4 bp) are often involved in end-joining events (Roth and Wilson 1986; Thacker *et al.* 1992; King *et al.* 1993; Sasaki *et al.* 2003) although it is not clearly established whether these events are the result of NHEJ or MMEJ. Soon after the experiments were performed in *yku70*Δ budding yeast cells, evidence for the conservation of MMEJ throughout evolution was provided by other studies in NHEJ-deficient cells from mammals (Kabotyanski *et al.* 1998; Feldmann *et al.* 2000; Zhong *et al.* 2002; Bentley *et al.* 2004; Guirouilh-Barbat *et al.* 2004; Tsuji *et al.* 2004), Arabidopsis (Heacock *et al.* 2004), *S. cerevisiae* (Ma *et al.* 2003; Yu and Gabriel 2003), and *S. pombe* (Manolis *et al.* 2001; Decottignies 2005). Moreover, biochemical purification approaches confirmed that enzymatic requirements for MMEJ are clearly distinct from NHEJ requirements in *Xenopus laevis* egg extracts (Gottlich *et al.* 1998).

Typical microhomologies at MMEJ junctions are 5–15 bp long and tend to be discontinuous, providing the opportunity for involvement of a DNA mismatch repair machinery in the process. Strikingly, MMEJ may be heavily oncogenic as suggested by recent studies establishing that an alternative DNA end-joining pathway is related to lymphomagenesis (Zhu *et al.* 2002; Tsuji *et al.* 2004) and liver cancer (Tong *et al.* 2002) in NHEJ-deficient mice and often leads to nonreciprocal translocations in either *Lig4*$^{-/-}$ or *Ku70*$^{-/-}$ mouse embryonic fibroblasts (Ferguson *et al.* 2000). Hence, MMEJ appears to act as a backup pathway to repair DNA when more accurate pathways have failed.

So far, genetic requirements for MMEJ have not been systematically investigated. The feature of nucleotide deletion formation at regions of microhomology in MMEJ is reminiscent of SSA, suggesting that genetic requirements for MMEJ and SSA may overlap. However, studies in Ku-deficient budding yeast cells showed that, although efficient MMEJ requires the *RAD1/RAD10* flap endonuclease needed for SSA (Ivanov and Haber 1995; Ma *et al.* 2003), it does not require *RAD52* (Yu and Gabriel 2003). In addition, although the Mre11 complex is largely dispensable for budding yeast SSA, it plays a role in plant MMEJ (Heacock *et al.* 2004) and is also involved in budding yeast MMEJ (Ma *et al.* 2003). Hence, it was suggested that SSA and MMEJ may represent distinct DNA repair mechanisms (Ma *et al.* 2003). On the other hand, another study performed in budding yeast established that extrachromosomal SSA acts with measurable efficiency in the presence of terminal direct repeats of only 10 bp, suggesting that the so-called MMEJ pathway may be related to SSA (Karathanasis and Wilson 2002). Hence, when this work was initiated, the nature of MMEJ was still unclear. To clarify the mechanism(s) underlying MMEJ, this study relied on the highly flexible PCR-based EC DSB repair assay established previously (Decottignies 2005). Although the chromatinization state of EC DNA may be different from the one encountered in a chromosomal break, data from budding yeast suggest that the ratio of HR/NHEJ events is highly similar in both types of DSB repair assays and that plasmid assays mirror chromosomal assays for other aspects of NHEJ and HR (SSA) regulation (Karathanasis and Wilson 2002).

Investigation of MMEJ genetic requirements was performed in fission yeast *lig4*Δ NHEJ-deficient cells. Genes involved in HR, NHEJ, *mis*match *r*epair (MMR), *n*ucleotide *e*xcision *r*epair (NER), and *b*ase *e*xcision *r*epair (BER) were chosen as putative candidate genes for MMEJ (Table 1). The EC DSB repair assay was also used to analyze the pattern of repair at mismatched nucleotides during MMEJ in the presence or absence of *msh2*$^{+}$. Finally, using a series of related MMEJ substrates, we investigated the inhibitory effect of Pku70 on fission yeast MMEJ unraveled in this study and the impact of both length and position of the microhomologous region on MMEJ efficiency.

MATERIALS AND METHODS

Fission yeast strains and methods: The *S. pombe* strains used in this study are described in Table 2. The *lig4*Δ*::LEU2* and *rad50*Δ*::LEU2* deletions (Tomita *et al.* 2003) were kindly provided by Masaru Ueno. The PN559 strain and the *rhp51*Δ*::kanR* and the *pku70*Δ*::kanR* (Baumann and Cech 2000) deletions were provided by Paul Nurse. Construction of the *pms1*Δ*::kanR*, *swi10*Δ*::kanR*, *rad16*Δ*::kanR*, *rad22*Δ*::kanR*, *rqh1*Δ*::kanR*, *pol4*Δ*::kanR*, *exo1*Δ*::kanR*, *rad2*Δ*::kanR*, *rad13*Δ*::kanR*, *spac12g12.16c*Δ*::kanR*, and *msh2*Δ*::kanR* alleles was adapted from Bahler *et al.* (1998). Briefly, two 100-bp-long PCR fragments comprising 80 bp of yeast genomic DNA located, respectively, upstream and downstream of the ORF (see supplemental file I at http://www.genetics.org/supplemental/ for primer sequences) were used as primers for PCR amplification of the *geneX*Δ*::kanR* cassettes on the pFA6a-kanMX6 plasmid. Genes were then deleted through homologous recombination after transformation of yeast with the *geneX*Δ*::kanR* PCR products.

Cells were cultured at 32° in rich glucose medium (YE5S) or Edinburgh minimal (EMM2) medium and sporulated on malt extract as described in Moreno *et al.* (1991). For nitrogen starvation, exponentially growing cells were pelleted, washed three times with water, and incubated at 2×10^6 cells/ml in EMM2 lacking NH_4Cl for 16 hr at 32°.

DNA for yeast transformations: The 1.7-kb *ura4*$^{+}$ (2+6) MMEJ substrate was PCR amplified with REP4 plasmid (Okazaki *et al.* 1990) as template and URAMMEJ5 and URAMMEJ3 as

TABLE 1

DNA repair genes included in this study

S. pombe gene	*S. cerevisiae* closest homolog	Function in *S. pombe*
lig4$^+$	*DNL4*	ATP-dependent DNA ligase involved in NHEJ (Baumann and Cech 2000)
pku70$^+$	*YKU70*	DNA-binding protein involved in DNA repair and telomere maintenance (Baumann and Cech 2000)
exo1$^+$	*EXO1*	5′ → 3′ exonuclease (XP-G family) involved in several DNA repair pathways such as MMR (Rudolph *et al.* 1998) and possibly HR (Tomita *et al.* 2003)
rad2$^+$	*RAD27*	ssDNA endonuclease (XP-G family) homologous to FEN-1; involved in mismatched DNA repair (Kunz and Fleck 2001) and telomere maintenance (Dahlen *et al.* 2003)
rad13$^+$	*RAD2*	ssDNA endonuclease (XP-G family) involved in NER (Kunz and Fleck 2001)
spac12g12.16c$^+$	*RAD27*	Member of the XP-G family of nucleases with unknown function
rad22$^+$	*RAD52*	Annealing of complementary single-stranded DNA; required for HR (Hegde *et al.* 1996; van den Bosch *et al.* 2001, 2002)
rhp51$^+$	*RAD51*	AAA ATPase with strand displacement activity involved in HR and telomere maintenance (Kibe *et al.* 2003)
rqh1$^+$	*SGS1*	DEAD/DEAH box DNA helicase (RecQ family) involved in HR-dependent DSB repair (Hegde *et al.* 1996)
msh2$^+$	*MSH2*	DNA mismatch repair protein (MutS homolog) required for MMR (Rudolph *et al.* 1998)
pms1$^+$	*PMS1*	DNA mismatch repair protein (MutL homolog) required for MMR (Rudolph *et al.* 1998)
swi10$^+$	*RAD10*	ssDNA repair endonuclease (ERCC1 family); forms a complex with Rad16 and is involved in NER (Carr *et al.* 1994; Rodel *et al.* 1997)
rad16$^+$	*RAD1*	ssDNA repair endonuclease (XP-F family); forms a complex with Swi10 and is involved in NER (Carr *et al.* 1994; Rodel *et al.* 1997)
pol4$^+$	*POL4*	PolX DNA polymerase with gap-filling activity; combines properties of mammalian DNA polymerase β, μ, and λ; possibly involved in BER and NHEJ (Gonzalez-Barrera *et al.* 2005)
rad50$^+$	*RAD50*	AAA ATPase involved in sister-chromatid recombination (Hartsuiker *et al.* 2001) and intermolecular NHEJ (Decottignies 2005)

primers. PCR amplifications were performed with Taq polymerase (Takara), implying the probable presence of nontemplated extra nucleotide(s) at the 3′-ends (Hu 1993). All primer sequences are listed in supplemental file II at http://www.genetics.org/supplemental/. MMEJ substrates for Figure 5B were PCR amplified with REP4 plasmid as template and the following primers: II, MMEJuraflap5 and URAMMEJ3; III, URAMMEJ5 and MMEJuraflap3; and IV, MMEJuraflap5 and MMEJuraflap3. MMEJ substrates from Figure 2B were obtained with the following primers: G/A, MMEJinv5 and MMEJinv3; and A/A, AAMMEJ5 and AAMMEJ3. The following primers were used to PCR amplify MMEJ substrates with varying lengths of microhomology (Figure 4): μ3, URAM3-5 and URAM3-3; μ4, URAM4-5 and URAM4-3; μ5, URAM5-5 and URAM5-3; μ6, URAM6-5 and URAM6-3; μ7, URAM7-5 and URAM7-3; μ8, URAM8-5 and URAM8-3. MMEJ substrates with varying distances between μ8 and the ends (Figure 5A) were obtained with the following primers: μ8(1), URAM8(1)-5 and URAM8(1)-3; μ8(3), URAM8(3)-5 and URAM8(3)-3; μ8(5), URAM8(5)-5 and URAM8(5)-3; and μ8(7), URAM8(7)-5 and URAM8(7)-3. Two micrograms of phenol/chloroform-purified DNA were used for each yeast transformation. Yeast transformations were performed using a protocol adapted from the lithium acetate method (Okazaki *et al.* 1990) described in Decottignies (2005). The number of Ura$^+$ colonies was scored after 4 days of incubation at 32°.

Identification of junctions in *ura4*$^+$ circles: Repair junctions were PCR amplified on boiled yeast colonies with IPCRURA1small and IPCRURA2. IPCRURA1 and IPCRURA2 primers were used to PCR amplify repair junctions from A/A substrate (Figure 2B). All primer sequences are listed in supplemental file II at http://www.genetics.org/supplemental/. PCR products were purified after agarose gel electrophoresis and sequenced using the DYEnamic sequencing kit from Amersham Biosciences.

RESULTS

Fission yeast MMEJ requires *rad22*+, *exo1*+, and *pol4*+ and is inhibited by *pku70*+: A previous study reported the formation of fission yeast Ura$^+$ colonies through NHEJ-mediated circularization of the PCR-amplified *ura4*$^+$ gene in *ura4-D18* cells (the *ura4-D18* mutation removes all homology with the transforming *ura4*$^+$ DNA substrate) (Decottignies 2005). NHEJ-deficient cells were also able to produce a few circular *ura4*$^+$ DNA molecules through MMEJ in the EC DSB repair assay (Decottignies 2005). Here, a modified *ura4*$^+$ repair substrate flanked by discontinuous microhomologous regions at both ends was PCR amplified and used to investigate genetic requirements for MMEJ in *lig4*Δ NHEJ-deficient cells (Figure 1A).

The GG**A**TTTGTA microhomologous region chosen consists of (2+6) overlapping nucleotides recovered previously in a subset of repair junctions in *lig4*Δ and/or *pku70*Δ NHEJ-deficient cells and containing one nonhomologous nucleotide (**A**) (Decottignies 2005). MMEJ-dependent circularization of the (2+6) *ura4*$^+$ repair substrate is thought to rely on a succession of steps (Figure 1A). First, DNA ends are subjected to 5′ → 3′ exonucleolytic degradation to produce complementary ssDNA

TABLE 2

Yeast strains used in this study

Strain	Genotype	Source
PN559	*h⁻ ura4-D18 leu1-32 ade6-M216*	P. Nurse
AD458	*h⁻ lig4Δ::LEU2 ura4-D18 leu1-32 ade6-M210*	This study
AD463	*h⁻ lig4Δ::LEU2 pku70Δ::kanR ura4-D18 leu1-32 his3-D1 ade6-M210*	This study
AD473	*h⁻ lig4Δ::LEU2 rad13Δ::kanR ura4-D18 leu1-32 ade6-M210*	This study
AD475	*h⁻ lig4Δ::LEU2 rad2Δ::kanR ura4-D18 leu1-32 ade6-M210*	This study
AD477	*h⁻ lig4Δ::LEU2 spac12g12.16cΔ::kanR ura4-D18 leu1-32 ade6-M210*	This study
AD479	*h⁺ lig4Δ::LEU2 pku70Δ::kanR rad50Δ::LEU2 ura4-D18 leu1-32 ade6-M216*	This study
AD486	*h⁺ lig4Δ::LEU2 pms1Δ::kanR ura4-D18 leu1-32 ade6-M210*	This study
AD487	*h⁺ lig4Δ::LEU2 msh2Δ::kanR ura4-D18 leu1-32 ade6-M210*	This study
AD493	*h⁻ lig4Δ::LEU2 swi10Δ::kanR ura4-D18 leu1-32 ade6-M210*	This study
AD501	*h⁻ lig4Δ::LEU2 pms1Δ::kanR swi10Δ::kanR ura4-D18 leu1-32 ade6-M210*	This study
AD503	*h⁻ lig4Δ::LEU2 exo1Δ::kanR ura4-D18 leu1-32 ade6-M210*	This study
AD511	*h⁻ lig4Δ::LEU2 rad16Δ::kanR ura4-D18 leu1-32 ade6-M210*	This study
AD512	*h⁻ lig4Δ::LEU2 rad22Δ::kanR ura4-D18 leu1-32 ade6-M210*	This study
AD516	*h⁻ exo1Δ::kanR ura4-D18 leu1-32 ade6-M216*	This study
AD518	*h⁻ lig4Δ::LEU2 rqh1Δ::kanR ura4-D18 leu1-32 ade6-M210*	This study
AD520	*h⁻ lig4Δ::LEU2 pol4Δ::kanR ura4-D18 leu1-32 ade6-M210*	This study
AD522	*h⁺ lig4Δ::LEU2 rhp51Δ::kanR ura4-D18*	This study
AD530	*h⁺ lig4Δ::LEU2 exo1Δ::kanR rhp51Δ::kanR ura4-D18 ade6-M216*	This study
AD535	*h⁺ lig4Δ::LEU2 rad50Δ::LEU2 ura4-D18 leu1-32 ade6-M210*	This study

sequences. After production of ssDNA, MMEJ proceeds through the search for homology and the annealing of complementary sequences. The next step probably consists of A/G mismatch correction within the microhomologous region. This mismatch was previously found to be corrected to A:T in 33 of 33 repair events isolated from NHEJ-deficient cells (Decottignies 2005). Finally, gaps are filled in and ligation seals the DNA ends. Circularization of PCR-amplified *ura4⁺* DNA was previously confirmed by Southern blot analysis (Decottignies 2005). In this study, absence of genomic integration of the (2+6) *ura4⁺* repair substrate was checked by monitoring Ura⁺ stability of both *lig4Δ* and *lig4Δpku70Δ* cells (supplemental file III at http://www.genetics.org/supplemental/).

To compare MMEJ efficiency in different *lig4Δ* genetic backgrounds, cells were transformed with either PCR-amplified *ura4⁺* DNA substrate (1.7 kb) or uncut REP4[*ura4⁺*] plasmid (8.5 kb).Circularization efficiency was calculated as the ratio of Ura⁺ colonies obtained after transformation with 2 μg of linear DNA substrate/Ura⁺ colonies obtained after transformation with 1 μg of circular REP4 plasmid (*ura4⁺* PCR/REP4 molar ratio of 10). A circularization efficiency of 3.2 ± 0.3% was measured in *lig4Δ* cells (Figure 1B). Under the same conditions (*ura4⁺* PCR/REP4 molar ratio of 10), circularization efficiency scored in wild-type (*lig4⁺*) cells amounted to ~250% (data not shown).

To test whether the production of ssDNA in the MMEJ process may be mediated by the Exo1 5′ → 3′ exonuclease, the *exo1⁺* gene was deleted in *lig4Δ* cells. Strikingly, MMEJ-dependent production of Ura⁺ colonies was almost completely abolished in *lig4Δexo1Δ* cells (circularization efficiency of 0.03 ± 0.02%) but *rad2⁺*, *rad13⁺*, and *spac12g12.16c⁺* were not required for EC MMEJ (Figure 1B). The annealing of complementary ssDNA sequences during the MMEJ repair process is probably achieved by Rad22 as no Ura⁺ colonies were recovered after transformation of *lig4Δrad22Δ* cells with *ura4⁺* DNA (circularization efficiency <0.03% with 95% confidence). It has been reported that *S. pombe rad22Δ* mutants are unstable and easily acquire suppressor mutations in the DNA helicase *fbh1⁺* gene (Doe *et al.* 2004; Osman *et al.* 2005). Accordingly, *lig4Δrad22Δ*-suppressed mutants appeared in the cultures and were MMEJ proficient in the EC DSB repair assay (data not shown). On the other hand, *rhp51⁺* and DNA helicase *rqh1⁺* were not required for MMEJ-dependent circularization of the (2+6) *ura4⁺* repair substrate (Figure 1B).

Next, the assay revealed that neither the impairment of MMR (*lig4Δmsh2Δ* or *lig4Δpms1Δ*) nor of NER (*lig4Δ swi10Δ*, *lig4Δrad16Δ*, or *lig4Δrad13Δ*), nor even of the combination of both (*lig4Δpms1Δswi10*) affected MMEJ efficiency (Figure 1B). Because of the gap-filling activity of fission yeast Pol4 (Gonzalez-Barrera *et al.* 2005), the MMEJ efficiency was also tested in *lig4Δpol4Δ* cells. As shown in Figure 1B, deletion of the *pol4⁺* gene abolished MMEJ-dependent repair of EC DSBs with discontinuous microhomologous ends (circularization efficiency <0.01% with 95% confidence). Finally, the EC repair assay was used to assess the impact of *pku70⁺* and *rad50⁺* genes on the MMEJ pathway. Strikingly, deletion of the *pku70⁺* gene increased MMEJ efficiency by fourfold, from 3.2 ± 0.3% to 13.1 ± 1.1%, suggesting that Pku70 is an inhibitor of MMEJ. On the other hand, deletion of *rad50⁺*, a gene encoding a subunit of the Mre11 complex, did not change MMEJ efficiency of either *lig4Δ* or *lig4Δpku70Δ* cells (Figure 1B).

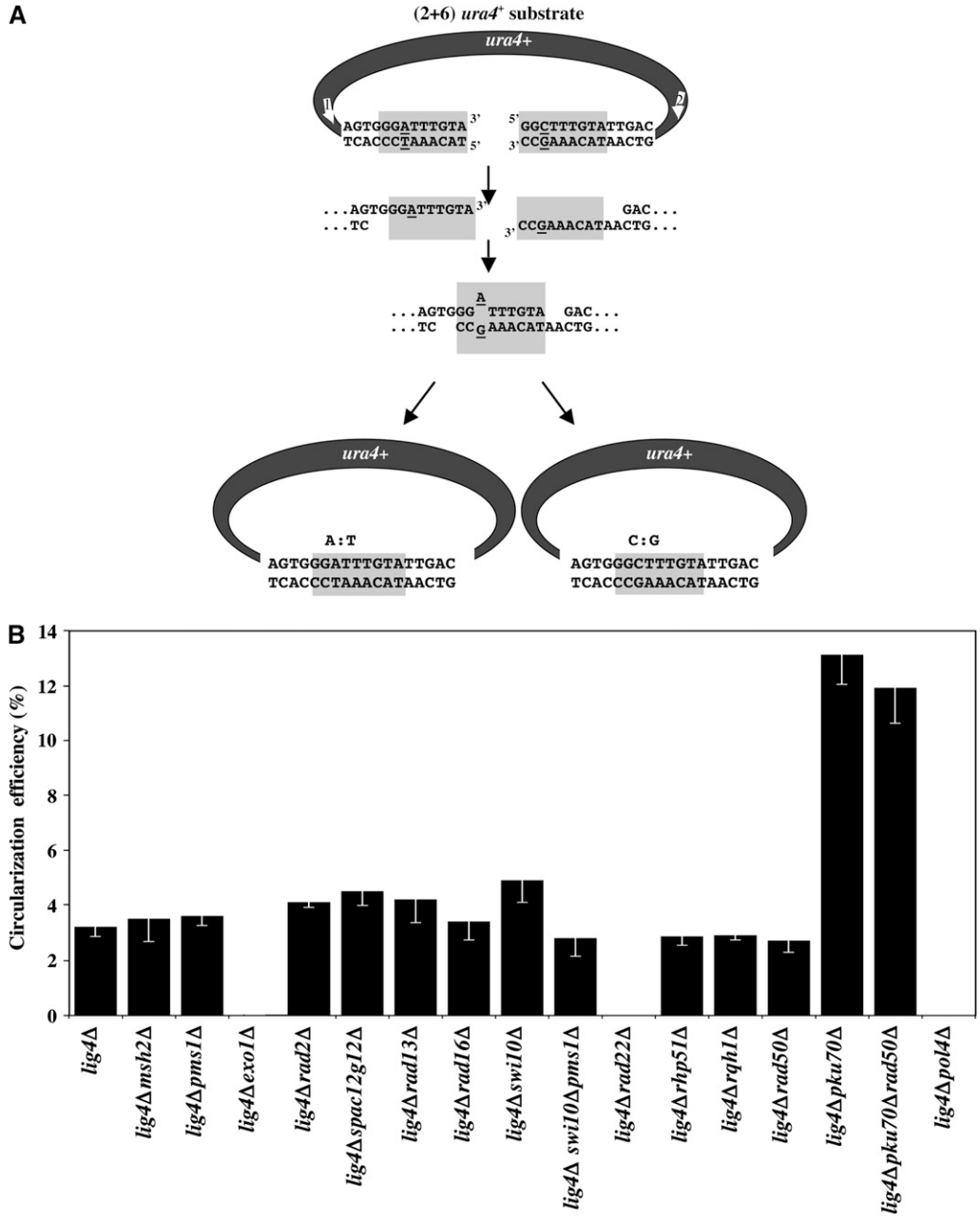

FIGURE 1.—Genetic requirements for fission yeast extrachromosomal MMEJ. (A) Presumed steps of MMEJ-dependent circularization of *ura4*$^+$ gene. Two distinct repair junction sequences are predicted to arise following A/G mismatch correction: A:T and C:G. Position of the primers used to amplify repair junctions is shown (1: IPCRURA1small; 2: IPCRURA2). (B) MMEJ efficiency was calculated as the ratio of Ura$^+$ colonies obtained after transformation with 2 μg (2+6) *ura4*$^+$ substrate/Ura$^+$ colonies scored after transformation with 1 μg REP4 plasmid (*ura4*$^+$ PCR/REP4 molar ratio of 10). Four to 10 independent yeast transformations were performed in each mutant background. Error bars represent the standard error of the mean (SEM).

Mismatch repair genes and mismatch type affect the pattern of MMEJ junctions: Although not required for circularization of *ura4*$^+$ DNA in the EC DSB repair assay (Figure 1B), Msh2 and Pms1 MMR proteins participate in the MMEJ process. Indeed, sequencing of the MMEJ repair junctions in *ura4*$^+$ circles revealed differences in the correction pattern of the putative A/G mismatch between *lig4*Δ and either *lig4*Δ*msh2*Δ or *lig4*Δ*pms1*Δ cells. In *lig4*Δ cells, 20 ± 2.4% of the repair junctions comprised a C:G nucleotide pair, A:T being detected in the remaining events (Figure 2, A and B). Deletion of the *rad2*$^+$, *spac12g12.16c*$^+$, *pku70*$^+$, or *rad50*$^+$ gene did not affect the pattern of repair junctions (Figure 2A). However, no C:G pair could be recovered from repair junctions in either *lig4*Δ*msh2*Δ or *lig4*Δ*pms1*Δ cells, suggesting that Pms1 and Msh2 MMR proteins may be involved in mismatch correction during the MMEJ process at discontinuous microhomologous regions. On the other hand, impairment of the NER pathway (*lig4*Δ*rad13*Δ or *lig4*Δ*swi10*Δ) did not change the C:G frequency at repair junctions. Surprisingly, a few C:G events (3.9 ± 0.6%) were recovered from *lig4*Δ*swi10*Δ*pms1*Δ cells, suggesting that inactivation of both NER and MMR pathways may activate a third mismatch repair pathway.

Strikingly, changing the putative mismatch from A/G to G/A within the microhomologous region, although not affecting circularization efficiency (2.8 ± 0.8% compared to 3.2 ± 0.3% in *lig4*Δ cells), resulted in the formation of G:C in, respectively, 94 ± 2.9% and 100% of the repair junctions in *lig4*Δ and *lig4*Δ*msh2*Δ cells (Figure

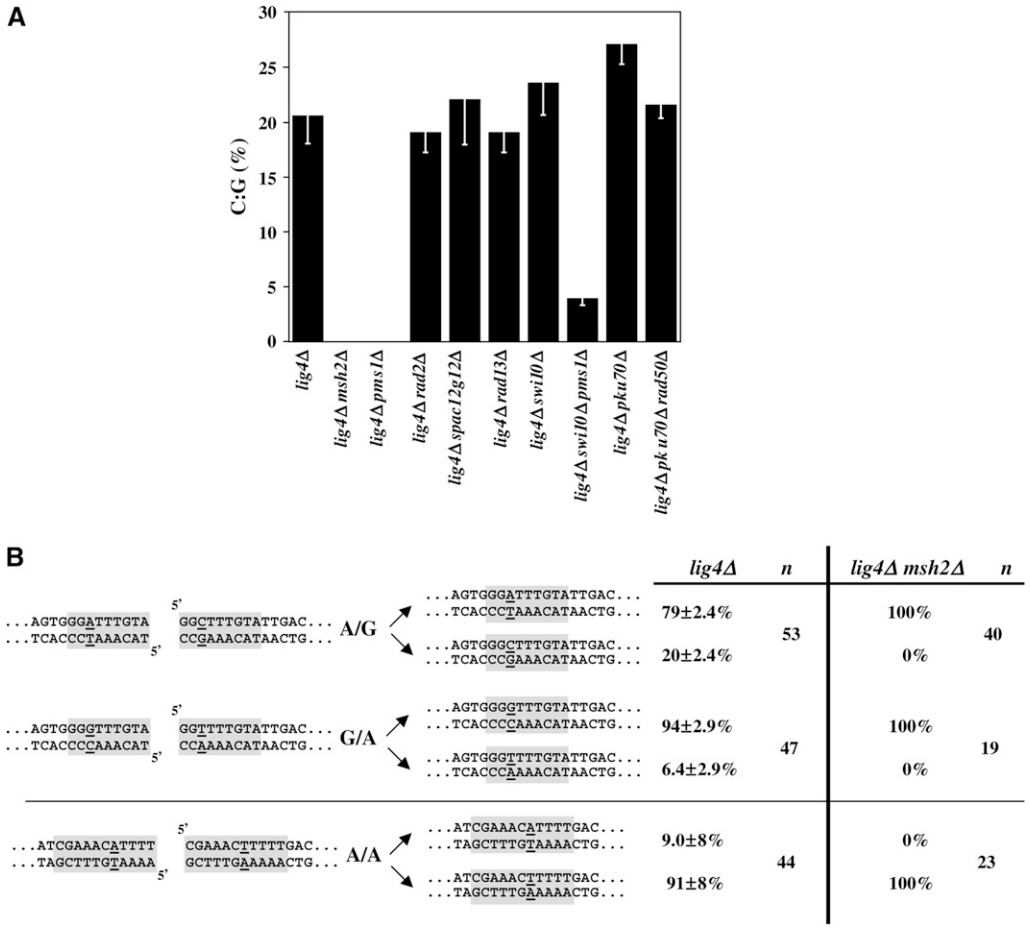

FIGURE 2.—Mismatch correction at MMEJ repair junctions. (A) The frequency of mismatch correction to C:G was calculated for MMEJ repair junction sequences recovered from three independent yeast transformations with (2+6) *ura4*$^+$ substrate. Error bars represent SEM. (B) MMEJ-associated mismatch correction was investigated in *lig4*Δ and *lig4*Δ*msh2*Δ cells following yeast transformation with *ura4*$^+$ substrates presenting the following mismatches during repair: A/G [(2+6) *ura4*$^+$], G/A, and A/A. Repair sequences were recovered from three independent yeast transformations (mean ± SEM). The total number of sequences analyzed is given under "*n*."

2B). Hence, with both MMEJ repair substrates, replacement of the nonhomologous nucleotide occurred mainly on the same strand (bottom strand in Figure 2B). Next, another repair substrate that involved the formation of a putative A/A mismatch within a completely different microhomologous region was tested (Figure 2B). In this case, replacement of the nonhomologous nucleotide occurred mainly on the top strand. All together, these data suggest that, during the EC MMEJ process, nucleotide replacement at the mismatched position can occur on either strand. However, with all three repair substrates tested, removal of the mismatched nucleotide occurred on the strand with the closer end, suggesting that the first mismatched nucleotide may be removed during slow 3′ → 5′ exonucleolytic digestion of the ends.

MMEJ and NHEJ are reciprocally regulated in G_1 cells: The inhibitory effect of Pku70 on EC MMEJ described above gives further evidence that NHEJ and MMEJ pathways rely on distinct machineries. Previous work reported that the fission yeast NHEJ level is 7- to 10-fold higher in nitrogen-starved G_1 cells compared to other cell cycle stages (FERREIRA and COOPER 2004). Hence, to test whether MMEJ and NHEJ may be distinctly regulated through the cell cycle, yeast cultures were enriched in G_1 cells by nitrogen starvation prior to transformation with *ura4*$^+$ DNA. The *lig4*Δ*pku70*Δ strain was chosen because of its high MMEJ efficiency.

As expected, G_1 arrest induced by nitrogen starvation in wild-type NHEJ-proficient cells increased the efficiency of Ura$^+$ colony formation sixfold compared to nonsynchronized cultures (Figure 3A). In contrast, circularization efficiency of *ura4*$^+$ DNA was decreased by more than a factor of 5 in nitrogen-starved *lig4*Δ*pku70*Δ cells compared to exponentially growing cells (mostly G_2 cells) (Figure 3A). Sequencing of repair junctions showed that the overlapping (2+6) microhomologous region was used for the repair in both G_1 and G_2 *lig4*Δ*pku70*Δ cells (not shown). Hence, these data suggest that NHEJ and MMEJ are reciprocally regulated through the cell cycle.

To test whether a decrease in exonuclease activity may be responsible for the reduced MMEJ efficiency in *lig4*Δ*pku70*Δ nitrogen-starved cells, cellular exonuclease activity in yeast nitrogen-starved cells was evaluated by sequencing NHEJ repair junctions recovered from wild-type G_1 cells (Figure 3, B and C). Consistent with a previous report in budding yeast (MOORE and HABER 1996), nucleotide deletion at repair junctions was increased in G_1 cells, suggesting that the reduced MMEJ efficiency measured in *lig4*Δ*pku70*Δ nitrogen-starved cells was not due to a lower level of exonuclease activity.

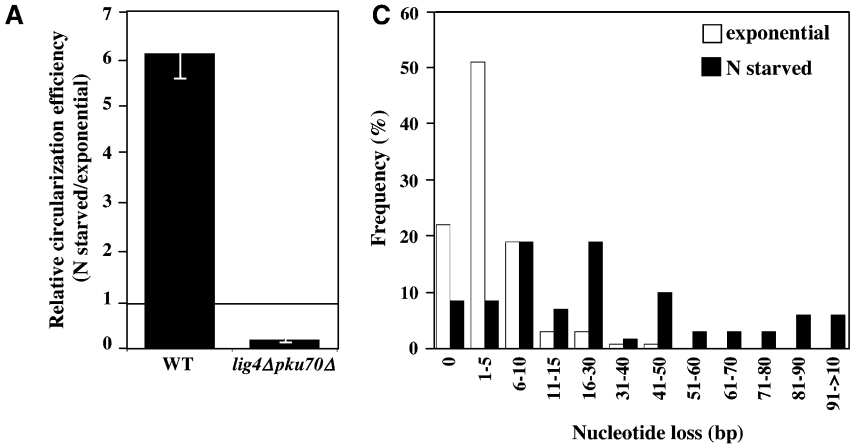

B

WT cells-nitrogen starvation

Junction	bp loss
ACTTTTTTAACACAAATGCATACATATAGCCAGTGGGATTTGTA GGCTTTGTATTGACGAAACTT	0
ACTTTTTTAACACAAATGCATACATATAGCCAGTGGGAT GGCTTTGTATTGACGAAACTT	5
ACTTTTTTAACACAAATGCATACATATAGCCAGTGGG GGCTTTGTATTGACGAAACTT	7
ACTTTTTTAACACAAATGCATACATATAGCCAGTGG **G** GCTTTGTATTGACGAAACTT	8
ACTTTTTTAACACAAATGCATACATATAGCC GGCTTTGTATTGACGAAACTT	13
AC GGCTTTGTATTGACGAAACTT	42
ACTTTTTTAACACAAATGCATACA GCTTTGTATTGACGAAACTT	21
ACTTTTTTAACACAAATGCATACATATAGCCAGTGGGATT CTTTGTATTGACGAAACTT	6
ACTTTTTTAACACAAATGCATACATATAGCCAGTGGGATT **T** TTGTATTGACGAAACTT	7
TATTGACGAAACTT	241
ACTTTTTTAACACAAATGCATACATATAGCCAGTGG TTGACGAAACTT	17
ACTTTTTTAACACAAATGCATACATATAGCCAGTGGGA **TT** GACGAAACTT	15
ACTTTTTTAACACAAATGCATACATATAGCCAGTGGGAT ACGAAACTT	17
ACTTTTTTAACACAAATGCATACATATAGCCAG CGAAACTT	24
CGAAACTT	127
ACTTTTTTAACACAAATGCATACATATAGC **C** GAAACTT	27
ACTTTTTTAACACAAATGCATACATATAGCCAGTG **GGATTTGTA** TTGACGAAACTT	9

FIGURE 3.—DSB repair in nitrogen-starved cells. (A) Circularization efficiency of (2+6) *ura4*$^+$ substrate through either NHEJ (WT-PN559) or MMEJ (*lig4*Δ*pku70*Δ) was measured after three independent yeast transformations of either nitrogen-starved or exponentially growing cells. Relative circularization efficiency was calculated as the ratio of efficiencies in nitrogen-starved/exponentially growing cells. See legend of Figure 1 for the circularization efficiency measurement. Error bars represent SEM. (B) Examples of DSB repair junctions recovered from transformation of nitrogen-starved wild-type (PN559) cells with (2+6) *ura4*$^+$ substrate. Microhomologous nucleotides are underlined. (C) A total of 63 DSB repair junctions recovered from exponentially growing wild-type (PN559) cells and 19 from nitrogen-starved wild-type cells were sequenced to determine nucleotide loss.

Pku70 increases the minimal microhomology length required for MMEJ: In NHEJ-deficient cells, the length of microhomologous regions recovered at DSB repair junctions extends from 3 to ~16 bp (BOULTON and JACKSON 1996; KABOTYANSKI *et al.* 1998; FELDMANN *et al.* 2000; MANOLIS *et al.* 2001; YU and GABRIEL 2003; DECOTTIGNIES 2005). To investigate the impact of microhomology length on the MMEJ-driven repair of DSBs, six *ura4*$^+$ repair substrates flanked by 3 to 8 homologous base pairs were obtained by PCR (μ3–μ8, Figure 4A). The presence of only 3 homologous base pairs was not enough to drive the MMEJ-dependent circularization of *ura4*$^+$ DNA (Figure 4B). Similarly, circularization of *ura4*$^+$ mediated through annealing at 4 or 5 homologous base pairs was still very inefficient in *lig4*Δ cells and amounted to, respectively, 0.06 ± 0.03% and 0.6 ± 0.1% (Figure 4B). However, circularization efficiency of μ5 substrate increased from 0.6 ± 0.1% to 19 ± 3.6% in *lig4*Δ*pku70*Δ cells, suggesting that 5 homologous base pairs are enough to drive detectable EC MMEJ in the absence of Pku70. In *lig4*Δ cells, significant MMEJ-dependent circularization was detected with μ6–μ8 substrates although efficiencies were always lower than the values obtained in *lig4*Δ*pku70*Δ cells (Figure 4B). Strikingly, circularization efficiency of μ8 substrate in *lig4*Δ*pku70*Δ cells (117 ± 10%) reaches ~50% of the NHEJ-dependent circularization efficiency of μ8 measured in *exo1*Δ cells (Figure 4C). However, although not affecting NHEJ-dependent circularization in *exo1*Δ cells, the presence of one mismatch within a microhomologous region comprising a total of eight overlapping nucleotides [(2+6) substrate] reduced EC MMEJ efficiency drastically in both *lig4*Δ and *lig4*Δ*pku70*Δ strains (Figure 4C).

Repair involving continuous microhomologies requires *rad22*+ but not *pol4*+: In contrast to the results obtained above with the MMEJ substrate showing discontinuous microhomologous sequences, the *pol4*$^+$ gene was found to be dispensable for Ura$^+$ colony formation after yeast transformation with μ5–μ8 substrates (Figure 4B). On the other hand, *rad22*$^+$ was found to be strictly required for EC MMEJ involving fewer than seven overlapping nucleotides, and repair efficiency was still very low with either μ7 or μ8 substrates (Figure 4B). Circularization efficiency of *lig4*Δ*exo1*Δ and *lig4*Δ*rhp51*Δ cells was intermediate between that of *lig4*Δ and *lig4*Δ*rad22*Δ strains, and deletion of both *exo1*$^+$ and *rhp51*$^+$ genes in *lig4*Δ cells abolished EC MMEJ activity (Figure 4B). These data suggest that both Rhp51-dependent and -independent HR mechanisms may be involved in the MMEJ repair process when continuous microhomologies are present.

Nonhomologous nucleotides at DNA ends reduce MMEJ efficiency: In DNA repair substrates used so far,

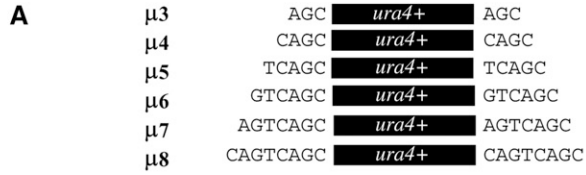

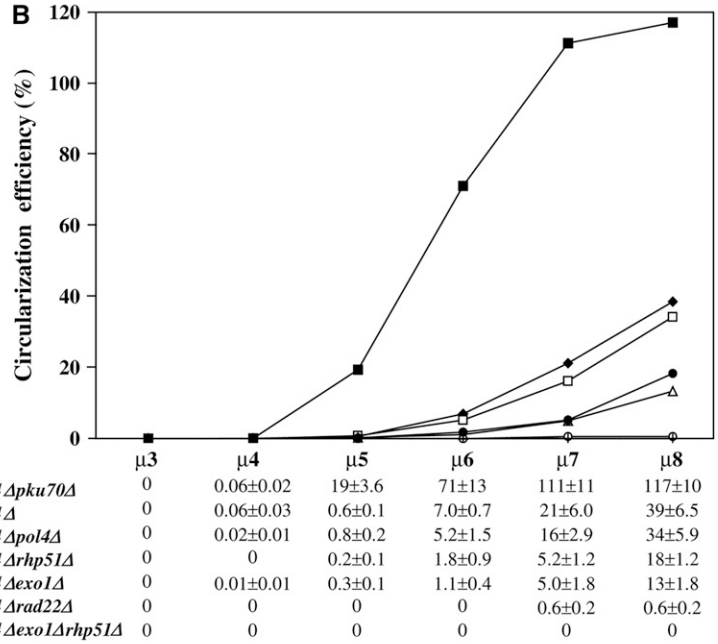

	μ3	μ4	μ5	μ6	μ7	μ8
lig4Δpku70Δ	0	0.06±0.02	19±3.6	71±13	111±11	117±10
lig4Δ	0	0.06±0.03	0.6±0.1	7.0±0.7	21±6.0	39±6.5
lig4Δpol4Δ	0	0.02±0.01	0.8±0.2	5.2±1.5	16±2.9	34±5.9
lig4Δrhp51Δ	0	0	0.2±0.1	1.8±0.9	5.2±1.2	18±1.2
lig4Δexo1Δ	0	0.01±0.01	0.3±0.1	1.1±0.4	5.0±1.8	13±1.8
lig4Δrad22Δ	0	0	0	0	0.6±0.2	0.6±0.2
lig4Δexo1Δrhp51Δ	0	0	0	0	0	0

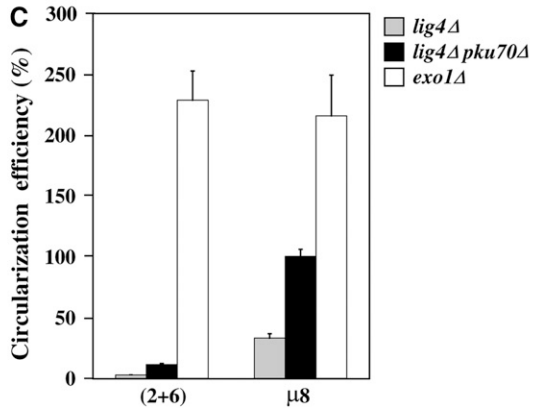

FIGURE 4.—Repair of DSBs with continuous microhomologies. (A and B) *ura4*$^+$ fragments with 3–8 terminal microhomologous base pairs were PCR amplified and used as EC MMEJ repair substrates in a series of *lig4*Δ derivatives. Circularization efficiency measurements with SEM (%) are detailed below the graph. (C) Circularization efficiencies of (2+6) and μ8 *ura4*$^+$ repair substrates were measured in *lig4*Δ, *lig4*Δ *pku70*Δ, and *exo1*Δ cells. Three to 10 independent yeast transformations were performed in each mutant background and circularization efficiencies were calculated as described in the Figure 1 legend. Error bars represent SEM.

microhomologous sequences are located at *ura4*$^+$ ends and are therefore directly accessible for MMEJ repair. However, microhomologous regions are often located away from the ends at naturally occurring DSBs, implying both extensive exonuclease degradation and 3′-flap removal for annealing at microhomologous regions. Hence, the effect of microhomology position on fission yeast EC MMEJ efficiency was tested by providing yeast cells with four derivatives of *ura4*$^+$ μ8 substrate containing increasing numbers of nonhomologous base pairs at both ends of the substrate [μ8(1), μ8(3), μ8(5), and μ8(7)] (Figure 5A). The presence of nonhomologous nucleotides did not change the efficiency of NHEJ-dependent circularization of *ura4*$^+$ in wild-type cells (data not shown). On the other hand, in *lig4*Δ cells, circularization of μ8 substrate was reduced by 63% in the presence of only 1 nonhomologous base pair at DNA ends [μ8(1)] and by 98% when 5 nonhomologous base pairs [μ8(5)] were added at both ends (Figure 5A).

Consistent with a protective role of Pku70 against exonucleases, circularization efficiency of μ8(1) was sixfold higher in *lig4*Δ*pku70*Δ cells compared to *lig4*Δ cells (Figure 5A). However, search for homology and/or removal of 3′-flap presumably became a limiting factor in *lig4*Δ*pku70*Δ cells transformed with either μ8(5) or μ8(7) substrate, suggesting that deprotection of DSB ends is not enough to promote efficient MMEJ in the presence of nonhomologous nucleotides (Figure 5A). Inactivation of Swi10/Rad16 endonuclease did not significantly affect circularization efficiency of *ura4*$^+$ DNA flanked by 1–7

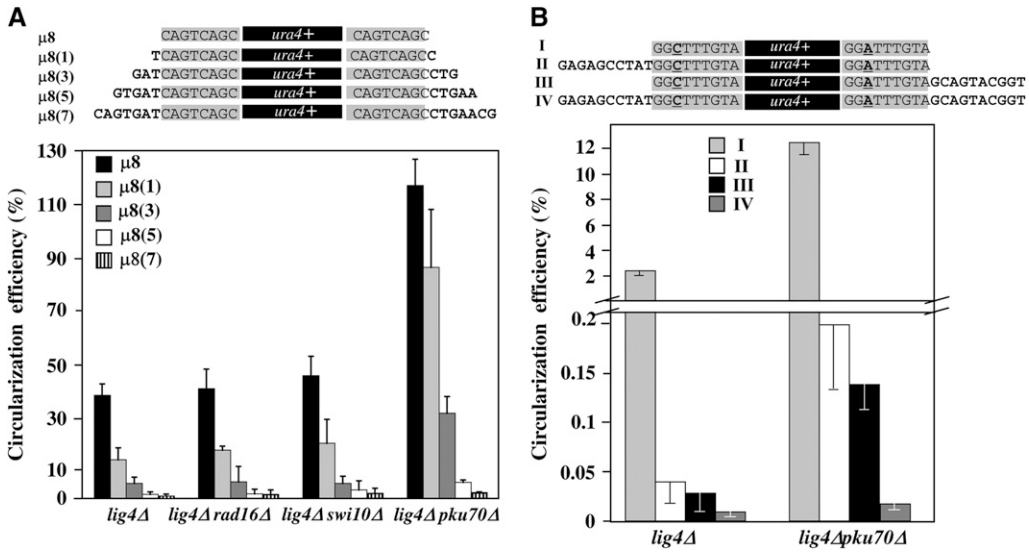

FIGURE 5.—Nonhomologous nucleotides at DSB ends reduce MMEJ efficiency. (A) Four derivatives of μ8 substrate flanked by 1 [μ8(1)], 3 [μ8(3)], 5 [μ8(5)], or 7 [μ8(7)] nonhomologous base pairs were PCR amplified and used as EC MMEJ repair substrates in *lig4*Δ, *lig4*Δ*rad16*Δ, *lig4*Δ*swi10*Δ, and *lig4*Δ*pku70*Δ cells. (B) Three derivatives of (2+6) repair substrate (I) containing 10 nonhomologous base pairs at the 5′-end (II), the 3′-end (III), or both ends (IV) were PCR amplified and introduced into *lig4*Δ and *lig4*Δ*pku70*Δ cells. Three to 10 independent yeast transformations were performed in each mutant background and circularization efficiencies were calculated as described in the Figure 1 legend. Error bars represent SEM.

nonhomologous base pairs (Figure 5A). Addition of nonhomologous base pairs at both ends of the (2+6) MMEJ substrate also drastically reduced *ura4*$^+$ circularization in NHEJ-deficient cells, suppressing the difference in MMEJ efficiency between *lig4*Δ and *lig4*Δ*pku70*Δ cells (Figure 5B). Similarly, nonhomologous base pairs at only one end of the PCR fragment strongly reduced the circularization efficiency (Figure 5B).

DISCUSSION

Recent studies suggested that MMEJ represents a nonconservative mechanism of DSB repair acting as backup pathway to NHEJ and is involved in oncogenic chromosomal translocations (FERGUSON *et al.* 2000; TONG *et al.* 2002; ZHU *et al.* 2002; TSUJI *et al.* 2004). MMEJ presumably proceeds through the resection of DSB ends to produce ssDNA tails overlapping at microhomologous regions of 5–15 nucleotides, a process reminiscent of SSA since repair results in a single copy of the repeated sequence (PAQUES and HABER 1999). Although microhomologies had been previously reported to help NHEJ-mediated repair of DSBs (ROTH and WILSON 1986; THACKER *et al.* 1992; KING *et al.* 1993; SASAKI *et al.* 2003), the MMEJ pathway is distinct from NHEJ because it does not rely on Ku and Lig4 NHEJ proteins for completion.

Hence, this study was aimed at investigating genetic requirements for MMEJ in fission yeast using an EC DSB repair assay described previously and based on the ability of fission yeast *ura4-D18* cells to acquire a Ura$^+$ phenotype through circularization of PCR-amplified *ura4*$^+$ DNA (DECOTTIGNIES 2005). Although EC DSBs are probably more accessible than DSBs encountered in a chromosomal context, resulting in higher repair efficiency, data from budding yeast suggest that EC assays mirror chromosomal breaks in several respects, including the ratio of HR/NHEJ repair events for a substrate flanked by 29-bp repeats (KARATHANASIS and WILSON 2002). The MMEJ repair substrates used in this study were obtained by PCR amplification of the *S. pombe ura4*$^+$ gene and were flanked by either noncontinuous (2+6) or continuous microhomologies of varying lengths (μ3–μ8). Fission yeast *lig4*Δ cells were able to circularize both types of MMEJ substrates provided that a continuous homology of at least 5 bp was present at the ends. When 8 homologous base pairs were available for *ura4*$^+$ circularization, EC MMEJ efficiency was very high, reaching up to 50% of the EC NHEJ efficiency. On the other hand, moving the microhomologous region, as few as 5 bp within the *ura4*$^+$ DNA fragment had a strong negative impact on MMEJ efficiency. However, MMEJ efficiency does not decrease further with increasing length of terminal nonhomologous base pairs as the efficiency measured in DECOTTIGNIES (2005) with the *ura4*$^+$ PCR substrate was comparable to that obtained here with μ8(5) and μ8(7) substrates, although in the former case terminal deletions of, respectively, 47 and 126 bp were required for annealing at the microhomologous region. Hence, above a threshold of ~5 bp, there is no further decrease in MMEJ efficiency with increasing lengths of nonhomologous 3′-flaps. This work is in agreement with data showing that moving the microhomologous region away from DSB ends substantially decreases the use of this region for DNA repair in mouse XRCC4-deficient cells (KABOTYANSKI *et al.* 1998) and reduces short homologous overlap-dependent

DNA recombination in Xenopus oocytes (Grzesiuk and Carroll 1987).

Fission yeast Rad22 is a homolog of budding yeast Rad52, a ssDNA-binding protein required for efficient annealing of complementary sequences in virtually all HR events, including SSA (Paques and Haber 1999). In this study, Rad22 was found to play a crucial role in EC MMEJ, being required for the formation of Ura^+ colonies after transformation with *ura4*$^+$ DNA flanked by either the (2+6) or a continuous microhomologous region. Requirement for Rad22 slightly decreased as the overlapping region size increased since a few Ura^+ colonies were recovered in *lig4*Δ*rad22*Δ cells transformed with DNA substrates bearing ≥7-bp-long continuous microhomologies. The MMEJ efficiency obtained with the μ8 substrate in *lig4*Δ*rad22*Δ cells (0.6%), however, was much lower than the one measured in *lig4*Δ cells (39%). Previous studies in budding yeast had concluded that Rad52 was not required for MMEJ as overlapping bases were present at DSB repair junctions in *yku70/80*Δ*rad52*Δ cells (Ma *et al.* 2003; Yu and Gabriel 2003) but, as suggested, Rad59, a Rad52 homolog important for SSA involving short homologous sequences (Sugawara *et al.* 2000; Davis and Symington 2001), may be important for budding yeast MMEJ (Yu and Gabriel 2003). On the other hand, using an EC DSB repair assay, another group reported that microhomologies of 10 bp are enough for budding yeast Rad52-mediated repair (Karathanasis and Wilson 2002).

Another gene that was found to be very important for fission yeast EC MMEJ is *exo1*$^+$. In *lig4*Δ*exo1*Δ cells, Ura^+ colonies were not recovered after transformation of *lig4*Δ*exo1*Δ cells with the (2+6) MMEJ substrate. Circularization efficiency in *lig4*Δ*exo1*Δ cells was also very low for *ura4*$^+$ molecules flanked by up to 6 microhomologous base pairs and threefold lower than the efficiency measured in *lig4*Δ cells when the μ8 substrate was used. Exo1 is a multi-tasking nuclease involved in budding yeast SSA and processing of DSBs in mitotic cells together with the Mre11 complex (Tran *et al.* 2004). In addition, budding and fission yeast Exo1 enzymes have been reported to participate in both MMR-dependent and MMR-independent mutation avoidance pathways, and *in vitro* studies showed that human EXO1 possesses a mismatch-dependent excision activity for both 5′ → 3′ and 3′ → 5′ excision tracts (Tran *et al.* 2004). Hence, the role of fission yeast Exo1 in MMEJ may be related to the production of ssDNA tails and/or to the excision of nonhomologous nucleotides when annealing occurs at regions of discontinuous microhomology. Notably, exonuclease activities of 5′ → 3′ and 3′ → 5′ directionality have been identified in the MMEJ fraction purified from *X. laevis* eggs by chromatography (Gottlich *et al.* 1998). The partial ability of *lig4*Δ*exo1*Δ cells to circularize the μ8 substrate suggests, however, that Exo1 exhibits functional redundancy with other exonuclease(s). Similarly, *lig4*Δ *rhp51*Δ cells showed reduced ability to circularize *ura4*$^+$ fragments flanked by continuous microhomologies. Deletion of both *exo1*$^+$ and *rhp51*$^+$ genes completely abolished μ8 circularization, suggesting that distinct HR mechanisms, both dependent on *rad22*$^+$, may be involved in MMEJ.

The *S. pombe pol4*$^+$ gene encodes a DNA polymerase belonging to the PolX family of polymerases devoted to DNA repair (Gonzalez-Barrera *et al.* 2005). Pol4 is template dependent, lacks a detectable 3′ → 5′ proofreading activity, and has a preference for small gaps. This study established that Pol4 is required for MMEJ-dependent circularization of *ura4*$^+$ DNA fragments with discontinuous microhomologies, suggesting that Pol4 may fill in the gaps after excision of nonhomologous nucleotides at overlapping junctions during MMEJ. In addition, Pol4 may also be involved in the base excision step itself through its deoxyribose phosphate lyase activity (Gonzalez-Barrera *et al.* 2005). These data agree with the requirement of budding yeast Pol4 for NHEJ-mediated processing and joining of DNA molecules with incompatible ends (Wilson and Lieber 1999; Tseng and Tomkinson 2004), including telomeric DNA (Pardo *et al.* 2006). Indeed, unlike *S. pombe*, budding yeast NHEJ is very inefficient at repairing DSBs with noncohesive ends and relies on the presence of microhomologies for NHEJ. Interestingly, mammalian Polμ, a PolX member, has also been proposed to function in microhomology-mediated NHEJ during V(D)J recombination (Ma *et al.* 2004; Nick McElhinny *et al.* 2005).

MMEJ-dependent circularization of *ura4*$^+$ DNA through discontinuous microhomologies presumably requires the intervention of a system able to recognize and correct mispaired bases. In *Escherichia coli*, the major pathway for mismatch correction during replication is the MutHLS pathway (Marti *et al.* 2002). In *S. pombe*, both *msh2*$^+$ and *msh6*$^+$ MutS homologs and the *pms1*$^+$ MutL homolog are central components of MMR, and their inactivation leads to increased mutation rates during vegetative growth and impaired mismatch correction during meiotic recombination (Marti *et al.* 2002). The NER pathway from *S. pombe* acts as another short-patch mismatch correction system that processes mismatches very efficiently in the absence of functional MMR (Marti *et al.* 2002). In this study, neither MMR nor NER pathways were strictly required for MMEJ-dependent circularization of *ura4*$^+$ (2+6) substrate, although the pattern of repair junction sequences of EC MMEJ substrates with discontinuous microhomologies was modified in the absence of the Msh2-dependent pathway. Although a homoduplex at repair junctions can also arise from a mismatch by replication, this work suggests the involvement of other repair pathways like the MMR-independent pathway of mutation avoidance associated with the *S. pombe exo1*$^+$ gene (Marti *et al.* 2002; Tran *et al.* 2004) and/or the BER pathway involving Pol4 (Gonzalez-Barrera *et al.* 2005).

This study further demonstrated that the fission yeast Mre11 complex is not required for EC MMEJ. However, studies in budding yeast and Arabidopsis had concluded

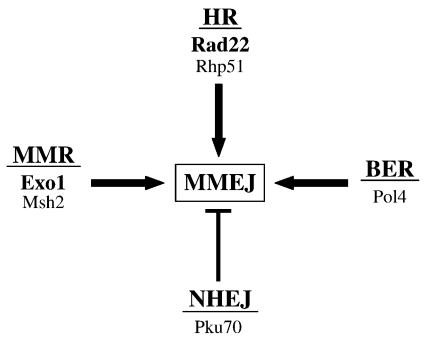

Figure 6.—Relationships among MMEJ, HR, NHEJ, and mismatch repair pathways in fission yeast. Rad22 and Exo1 proteins are required for EC MMEJ, suggesting that MMEJ is related to SSA. Rhp51 is involved in EC MMEJ only if continuous microhomologies are available for the repair. Pol4 is strictly required for repair involving the use of discontinuous microhomologies. Msh2 MMR protein is also involved in EC MMEJ at discontinuous microhomologous regions. Both types of EC MMEJ (continuous/discontinuous microhomologies) are inhibited by Pku70.

that inactivation of the Mre11 complex reduces MMEJ efficiency (Yu and Gabriel 2003; Heacock *et al.* 2004). It was previously established that the fission yeast Mre11 complex is important for intermolecular ligation events during EC NHEJ (Decottignies 2005). Hence, the apparent discrepancy between the results may be related to the experimental design as both budding yeast and Arabidopsis studies looked at intermolecular MMEJ events in a chromosomal context while this study focused on intramolecular MMEJ at the extrachromosomal level.

Pku70 was a strong inhibitor of EC MMEJ. Stimulation of MMEJ efficiency upon *pku70*$^+$ gene deletion was higher with shorter microhomology lengths, going from threefold if 8 homologous base pairs were available for MMEJ to 30-fold in the presence of 5 homologous base pairs. Hence, it appears that short microhomologies of 5–6 bp may not be enough for MMEJ repair to compete with Pku70. The influence of Pku70 was still detectable when the microhomologous region was moved inside the DNA by the addition of up to 3 nonhomologous base pairs at *ura4*$^+$ ends. These data support a protective role for the Ku heterodimer, which, by binding to DNA ends, presumably reduces access to exonucleases (Getts and Stamato 1994), thereby limiting the MMEJ process. Together with the work in *S. cerevisae* showing that the error-prone repair of DSBs with noncohesive ends is facilitated by deletion of *KU70* (Boulton and Jackson 1996), this study supports a role for Ku in repressing MMEJ-dependent repair of DSBs. Since recent studies suggest that Ku heterodimer helps maintain genome integrity by suppressing an alternative repair pathway that leads to chromosomal translocations in mammals (Difilippantonio *et al.* 2000; Ferguson *et al.* 2000; Tong *et al.* 2002), one can postulate that, in mammalian cells, Ku may also suppress MMEJ-dependent chromosomal translocations.

The genetic requirements for MMEJ unraveled in this study suggest that MMEJ acts as a backup pathway of NHEJ that uses components of other DNA repair pathways to mediate error-prone end joining (Figure 6). Hence, MMEJ does not represent a new DNA repair pathway but is related to HR. Accordingly, MMEJ efficiency was reduced in G_1-arrested cells, a cell cycle stage characterized by low HR activity (Lisby *et al.* 2001; Ferreira and Cooper 2004). In favor of this hypothesis, previous studies in budding yeast (Mezard *et al.* 1992; Karathanasis and Wilson 2002) and Xenopus oocytes (Grzesiuk and Carroll 1987) suggested that EC DSB repair involving the use of very short stretches of identity (<10 bp) was mediated by the HR machinery. Requirement for Rad22 and Exo1 suggests that MMEJ may proceed similarly to SSA. Moreover, involvement of Msh2 and Pms1 in fission yeast EC MMEJ repair agrees with the reduction in SSA-associated mismatch repair observed in both *pms1* and *msh2* mutant budding yeast cells (Sugawara *et al.* 2004). The Rad16/Swi10 complex homologous to Rad1/Rad10, a ssDNA-specific endonuclease playing a crucial role in budding yeast SSA (Ivanov and Haber 1995), was not required for fission yeast EC MMEJ. However, lack of Rad16/Swi10 dependency in this study is in agreement with the observation that budding yeast Rad1/Rad10 endonuclease is not required for the removal of 3′-tails shorter than 30 nucleotides (Paques and Haber 1997). Altogether, these data indicate that MMEJ operates through SSA. Hence, the name "micro-SSA" may be more appropriate for this type of repair to avoid confusion with NHEJ, a Lig4-dependent DNA repair pathway for which a subset of events also involves the use of microhomologies.

Previous study in budding yeast reported that SSA occurs with flanking homologous sequences as small as 10 bp (Sugawara *et al.* 2000; Karathanasis and Wilson 2002); this work suggests that 5 bp of homology may be enough, at least in an extrachromosomal context. The minimal microhomology length, however, may be higher in a chromosomal context. On the other hand, since significant MMEJ efficiency in *lig4*Δ*pku70*Δ cells was obtained only for *ura4*$^+$ DNA fragments bearing terminal continuous microhomologies of at least 5 bp, this work suggests that the very short homologous sequences of 1–4 bp frequently detected at DSB repair junctions of NHEJ-proficient cells (Roth and Wilson 1986; Schiestl and Petes 1991; Thacker *et al.* 1992; King *et al.* 1993; Manivasakam *et al.* 1995) may reflect a distinct process and possibly result from Ku-dependent NHEJ activity. In that respect, crystal structure of the Ku heterodimer suggests that Ku may confine DNA movement to a helical path, creating a complex that may help the search for short complementary sequences (Walker *et al.* 2001).

I am grateful to P. Nurse and M. Ueno for the gift of strains. I thank members of the Ludwig Institute of Cancer Research (Brussels) for stimulating discussions. This work was supported by the Fonds National de la Recherche Scientifique (Belgium).

LITERATURE CITED

Bahler, J., J. Q. Wu, M. S. Longtine, N. G. Shah, A. McKenzie, III *et al.*, 1998 Heterologous modules for efficient and versatile PCR-based gene targeting in Schizosaccharomyces pombe. Yeast **14:** 943–951.

Baumann, P., and T. R. Cech, 2000 Protection of telomeres by the Ku protein in fission yeast. Mol. Biol. Cell **11:** 3265–3275.

Bentley, J., C. P. Diggle, P. Harnden, M. A. Knowles and A. E. Kiltie, 2004 DNA double strand break repair in human bladder cancer is error prone and involves microhomology-associated end-joining. Nucleic Acids Res. **32:** 5249–5259.

Boulton, S. J., and S. P. Jackson, 1996 Saccharomyces cerevisiae Ku70 potentiates illegitimate DNA double-strand break repair and serves as a barrier to error-prone DNA repair pathways. Embo J. **15:** 5093–5103.

Carr, A. M., H. Schmidt, S. Kirchhoff, W. J. Muriel, K. S. Sheldrick *et al.*, 1994 The rad16 gene of Schizosaccharomyces pombe: a homolog of the RAD1 gene of Saccharomyces cerevisiae. Mol. Cell. Biol. **14:** 2029–2040.

Dahlen, M., P. Sunnerhagen and T. S. Wang, 2003 Replication proteins influence the maintenance of telomere length and telomerase protein stability. Mol. Cell. Biol. **23:** 3031–3042.

D'Amours, D., and S. P. Jackson, 2002 The Mre11 complex: at the crossroads of DNA repair and checkpoint signalling. Nat. Rev. Mol. Cell Biol. **3:** 317–327.

Davis, A. P., and L. S. Symington, 2001 The yeast recombinational repair protein Rad59 interacts with Rad52 and stimulates single-strand annealing. Genetics **159:** 515–525.

Davis, A. P., and L. S. Symington, 2004 RAD51-dependent break-induced replication in yeast. Mol. Cell. Biol. **24:** 2344–2351.

Decottignies, A., 2005 Capture of extranuclear DNA at fission yeast double-strand breaks. Genetics **171:** 1535–1548.

Difilippantonio, M. J., J. Zhu, H. T. Chen, E. Meffre, M. C. Nussenzweig *et al.*, 2000 DNA repair protein Ku80 suppresses chromosomal aberrations and malignant transformation. Nature **404:** 510–514.

Doe, C. L., F. Osman, J. Dixon and M. C. Whitby, 2004 DNA repair by a Rad22-Mus81-dependent pathway that is independent of Rhp51. Nucleic Acids Res. **32:** 5570–5581.

Feldmann, E., V. Schmiemann, W. Goedecke, S. Reichenberger and P. Pfeiffer, 2000 DNA double-strand break repair in cell-free extracts from Ku80-deficient cells: implications for Ku serving as an alignment factor in non-homologous DNA end joining. Nucleic Acids Res. **28:** 2585–2596.

Ferguson, D. O., J. M. Sekiguchi, S. Chang, K. M. Frank, Y. Gao *et al.*, 2000 The nonhomologous end-joining pathway of DNA repair is required for genomic stability and the suppression of translocations. Proc. Natl. Acad. Sci. USA **97:** 6630–6633.

Ferreira, M. G., and J. P. Cooper, 2004 Two modes of DNA double-strand break repair are reciprocally regulated through the fission yeast cell cycle. Genes Dev. **18:** 2249–2254.

Getts, R. C., and T. D. Stamato, 1994 Absence of a Ku-like DNA end binding activity in the xrs double-strand DNA repair-deficient mutant. J. Biol. Chem. **269:** 15981–15984.

Gonzalez-Barrera, S., A. Sanchez, J. F. Ruiz, R. Juarez, A. J. Picher *et al.*, 2005 Characterization of SpPol4, a unique X-family DNA polymerase in Schizosaccharomyces pombe. Nucleic Acids Res. **33:** 4762–4774.

Gottlich, B., S. Reichenberger, E. Feldmann and P. Pfeiffer, 1998 Rejoining of DNA double-strand breaks in vitro by single-strand annealing. Eur. J. Biochem. **258:** 387–395.

Grzesiuk, E., and D. Carroll, 1987 Recombination of DNAs in Xenopus oocytes based on short homologous overlaps. Nucleic Acids Res. **15:** 971–985.

Guirouilh-Barbat, J., S. Huck, P. Bertrand, L. Pirzio, C. Desmaze *et al.*, 2004 Impact of the KU80 pathway on NHEJ-induced genome rearrangements in mammalian cells. Mol. Cell **14:** 611–623.

Hartsuiker, E., E. Vaessen, A. M. Carr and J. Kohli, 2001 Fission yeast Rad50 stimulates sister chromatid recombination and links cohesion with repair. EMBO J. **20:** 6660–6671.

Heacock, M., E. Spangler, K. Riha, J. Puizina and D. E. Shippen, 2004 Molecular analysis of telomere fusions in Arabidopsis: multiple pathways for chromosome end-joining. EMBO J. **23:** 2304–2313.

Hegde, V., R. J. McFarlane, E. M. Taylor and C. Price, 1996 The genetics of the repair of 5-azacytidine-mediated DNA damage in the fission yeast Schizosaccharomyces pombe. Mol. Gen. Genet. **251:** 483–492.

Hu, G., 1993 DNA polymerase-catalyzed addition of nontemplated extra nucleotides to the 3′ end of a DNA fragment. DNA Cell Biol. **12:** 763–770.

Ivanov, E. L., and J. E. Haber, 1995 RAD1 and RAD10, but not other excision repair genes, are required for double-strand break-induced recombination in Saccharomyces cerevisiae. Mol. Cell. Biol. **15:** 2245–2251.

Jackson, S. P., 2002 Sensing and repairing DNA double-strand breaks. Carcinogenesis **23:** 687–696.

Kabotyanski, E. B., L. Gomelsky, J. O. Han, T. D. Stamato and D. B. Roth, 1998 Double-strand break repair in Ku86- and XRCC4-deficient cells. Nucleic Acids Res. **26:** 5333–5342.

Karathanasis, E., and T. E. Wilson, 2002 Enhancement of *Saccharomyces cerevisiae* end-joining efficiency by cell growth stage but not by impairment of recombination. Genetics **161:** 1015–1027.

Kibe, T., K. Tomita, A. Matsuura, D. Izawa, T. Kodaira *et al.*, 2003 Fission yeast Rhp51 is required for the maintenance of telomere structure in the absence of the Ku heterodimer. Nucleic Acids Res. **31:** 5054–5063.

King, J. S., E. R. Valcarcel, J. T. Rufer, J. W. Phillips and W. F. Morgan, 1993 Noncomplementary DNA double-strand-break rejoining in bacterial and human cells. Nucleic Acids Res. **21:** 1055–1059.

Kunz, C., and O. Fleck, 2001 Role of the DNA repair nucleases Rad13, Rad2 and Uve1 of Schizosaccharomyces pombe in mismatch correction. J. Mol. Biol. **313:** 241–253.

Lisby, M., R. Rothstein and U. H. Mortensen, 2001 Rad52 forms DNA repair and recombination centers during S phase. Proc. Natl. Acad. Sci. USA **98:** 8276–8282.

Ma, J. L., E. M. Kim, J. E. Haber and S. E. Lee, 2003 Yeast Mre11 and Rad1 proteins define a Ku-independent mechanism to repair double-strand breaks lacking overlapping end sequences. Mol. Cell. Biol. **23:** 8820–8828.

Ma, Y., H. Lu, B. Tippin, M. F. Goodman, N. Shimazaki *et al.*, 2004 A biochemically defined system for mammalian nonhomologous DNA end joining. Mol. Cell **16:** 701–713.

Manivasakam, P., S. C. Weber, J. McElver and R. H. Schiestl, 1995 Micro-homology mediated PCR targeting in Saccharomyces cerevisiae. Nucleic Acids Res. **23:** 2799–2800.

Manolis, K. G., E. R. Nimmo, E. Hartsuiker, A. M. Carr, P. A. Jeggo *et al.*, 2001 Novel functional requirements for non-homologous DNA end joining in Schizosaccharomyces pombe. EMBO J. **20:** 210–221.

Marti, T. M., C. Kunz and O. Fleck, 2002 DNA mismatch repair and mutation avoidance pathways. J. Cell. Physiol. **191:** 28–41.

Mezard, C., D. Pompon and A. Nicolas, 1992 Recombination between similar but not identical DNA sequences during yeast transformation occurs within short stretches of identity. Cell **70:** 659–670.

Moore, J. K., and J. E. Haber, 1996 Cell cycle and genetic requirements of two pathways of nonhomologous end-joining repair of double-strand breaks in Saccharomyces cerevisiae. Mol. Cell. Biol. **16:** 2164–2173.

Moreno, S., A. Klar and P. Nurse, 1991 Molecular genetic analysis of fission yeast Schizosaccharomyces pombe. Methods Enzymol. **194:** 795–823.

Nick McElhinny, S. A., J. M. Havener, M. Garcia-Diaz, R. Juarez, K. Bebenek *et al.*, 2005 A gradient of template dependence defines distinct biological roles for family X polymerases in nonhomologous end joining. Mol. Cell **19:** 357–366.

Okazaki, K., N. Okazaki, K. Kume, S. Jinno, K. Tanaka *et al.*, 1990 High-frequency transformation method and library transducing vectors for cloning mammalian cDNAs by trans-complementation of Schizosaccharomyces pombe. Nucleic Acids Res. **18:** 6485–6489.

Osman, F., J. Dixon, A. R. Barr and M. C. Whitby, 2005 The F-Box DNA helicase Fbh1 prevents Rhp51-dependent recombination without mediator proteins. Mol. Cell. Biol. **25:** 8084–8096.

Ozenberger, B. A., and G. S. Roeder, 1991 A unique pathway of double-strand break repair operates in tandemly repeated genes. Mol. Cell. Biol. **11:** 1222–1231.

Paques, F., and J. E. Haber, 1997 Two pathways for removal of nonhomologous DNA ends during double-strand break repair in Saccharomyces cerevisiae. Mol. Cell. Biol. **17:** 6765–6771.

Paques, F., and J. E. Haber, 1999 Multiple pathways of recombination induced by double-strand breaks in Saccharomyces cerevisiae. Microbiol. Mol. Biol. Rev. **63:** 349–404.

Pardo, B., E. Ma and S. Marcand, 2006 Mismatch tolerance by DNA polymerase Pol4 in the course of nonhomologous end joining in *Saccharomyces cerevisiae*. Genetics **172:** 2689–2694.

Rodel, C., T. Jupitz and H. Schmidt, 1997 Complementation of the DNA repair-deficient swi10 mutant of fission yeast by the human ERCC1 gene. Nucleic Acids Res. **25:** 2823–2827.

Roth, D. B., and J. H. Wilson, 1986 Nonhomologous recombination in mammalian cells: role for short sequence homologies in the joining reaction. Mol. Cell. Biol. **6:** 4295–4304.

Rudolph, C., O. Fleck and J. Kohli, 1998 Schizosaccharomyces pombe exo1 is involved in the same mismatch repair pathway as msh2 and pms1. Curr. Genet. **34:** 343–350.

Sasaki, S., Y. Kitagawa, Y. Sekido, J. D. Minna, H. Kuwano *et al.*, 2003 Molecular processes of chromosome 9p21 deletions in human cancers. Oncogene **22:** 3792–3798.

Schiestl, R. H., and T. D. Petes, 1991 Integration of DNA fragments by illegitimate recombination in Saccharomyces cerevisiae. Proc. Natl. Acad. Sci. USA **88:** 7585–7589.

Shen, P., and H. V. Huang, 1986 Homologous recombination in *Escherichia coli*: dependence on substrate length and homology. Genetics **112:** 441–457.

Sugawara, N., G. Ira and J. E. Haber, 2000 DNA length dependence of the single-strand annealing pathway and the role of Saccharomyces cerevisiae RAD59 in double-strand break repair. Mol. Cell. Biol. **20:** 5300–5309.

Sugawara, N., T. Goldfarb, B. Studamire, E. Alani and J. E. Haber, 2004 Heteroduplex rejection during single-strand annealing requires Sgs1 helicase and mismatch repair proteins Msh2 and Msh6 but not Pms1. Proc. Natl. Acad. Sci. USA **101:** 9315–9320.

Thacker, J., J. Chalk, A. Ganesh and P. North, 1992 A mechanism for deletion formation in DNA by human cell extracts: the involvement of short sequence repeats. Nucleic Acids Res. **20:** 6183–6188.

Tomita, K., A. Matsuura, T. Caspari, A. M. Carr, Y. Akamatsu *et al.*, 2003 Competition between the Rad50 complex and the Ku heterodimer reveals a role for Exo1 in processing double-strand breaks but not telomeres. Mol Cell Biol **23:** 5186–5197.

Tong, W. M., U. Cortes, M. P. Hande, H. Ohgaki, L. R. Cavalli *et al.*, 2002 Synergistic role of Ku80 and poly(ADP-ribose) polymerase in suppressing chromosomal aberrations and liver cancer formation. Cancer Res. **62:** 6990–6996.

Tran, P. T., N. Erdeniz, L. S. Symington and R. M. Liskay, 2004 EXO1-A multi-tasking eukaryotic nuclease. DNA Rep. **3:** 1549–1559.

Tseng, H. M., and A. E. Tomkinson, 2004 Processing and joining of DNA ends coordinated by interactions among Dnl4/Lif1, Pol4, and FEN-1. J. Biol. Chem. **279:** 47580–47588.

Tsuji, H., H. Ishii-Ohba, T. Katsube, H. Ukai, S. Aizawa *et al.*, 2004 Involvement of illegitimate V(D)J recombination or microhomology-mediated nonhomologous end-joining in the formation of intragenic deletions of the Notch1 gene in mouse thymic lymphomas. Cancer Res. **64:** 8882–8890.

van den Bosch, M., K. Vreeken, J. B. Zonneveld, J. A. Brandsma, M. Lombaerts *et al.*, 2001 Characterization of RAD52 homologs in the fission yeast Schizosaccharomyces pombe. Mutat. Res. **461:** 311–323.

van den Bosch, M., J. B. Zonneveld, K. Vreeken, F. A. de Vries, P. H. Lohman *et al.*, 2002 Differential expression and requirements for Schizosaccharomyces pombe RAD52 homologs in DNA repair and recombination. Nucleic Acids Res. **30:** 1316–1324.

Walker, J. R., R. A. Corpina and J. Goldberg, 2001 Structure of the Ku heterodimer bound to DNA and its implications for double-strand break repair. Nature **412:** 607–614.

Wilson, T. E., and M. R. Lieber, 1999 Efficient processing of DNA ends during yeast nonhomologous end joining. Evidence for a DNA polymerase beta (Pol4)-dependent pathway. J. Biol. Chem. **274:** 23599–23609.

Yu, X., and A. Gabriel, 2003 Ku-dependent and Ku-independent end-joining pathways lead to chromosomal rearrangements during double-strand break repair in *Saccharomyces cerevisiae*. Genetics **163:** 843–856.

Zhong, Q., C. F. Chen, P. L. Chen and W. H. Lee, 2002 BRCA1 facilitates microhomology-mediated end joining of DNA double strand breaks. J. Biol. Chem. **277:** 28641–28647.

Zhu, C., K. D. Mills, D. O. Ferguson, C. Lee, J. Manis *et al.*, 2002 Unrepaired DNA breaks in p53-deficient cells lead to oncogenic gene amplification subsequent to translocations. Cell **109:** 811–821.

Communicating editor: G. R. Smith